

MR-ARFI and SWI to Detect Calcifications in the Brain in MRgHIFU Treatments

R. R. Bitton¹, E. Kaye^{1,2}, and K. Butts Pauly¹

¹Radiology, Stanford University, Stanford, CA, United States, ²Electrical Engineering, Stanford University, Stanford, CA, United States

Introduction

Calcifications in the brain can be associated with several intracranial pathologies including tumor growth, epilepsy, hyperthyroidism, and infectious diseases [1][2]. Recent advances have shown that MR guided High Intensity Focused Ultrasound (MRgHIFU) can be used in the brain, as a non-invasive functional neurosurgery [3]. Calcifications exhibit a high acoustic attenuation coefficient compared with surrounding brain tissue thus, having the potential to interfere with an MRgHIFU treatment. Prostate cancer HIFU studies have deemed major prostatic calcifications a contraindication to prostate HIFU treatment [4]. For these reasons, it is of interest to visualize the presence of calcifications in brain during an MRgHIFU treatment. While calcifications may be identified in pre-treatment CT scans, they are not registered to the MR images or the in vivo HIFU focal spot. SWI has identified calcifications in the brain by exploiting the diamagnetic properties of calcium, although problems of aliasing and overestimation of size exist [5]. Additionally, MR-Acoustic Radiation Force Imaging (MR-ARFI) can exploit the ultrasonic interaction with calcium by mapping local displacements, and has been explored in phantoms [6]. In this study we present the use MR-ARFI imaging to detect a calcification in ex-vivo swine brain by creating a displacement weighted map of an ROI larger than the focal spot. This technique is proposed as an adjunct to SWI in order to visualize calcifications.

Methods

The MR-ARFI was performed in a GE 3T scanner using the InSightec ExAblate 2000 system with a solenoid breast coil. Calcium hydroxyapatite particles (0.8-1.8mm diameter) were placed in a whole ex-vivo swine brain. A CT image shows the experimental setup (Fig 1), and was used to validate the calcification location. The density is measured in Hounsfield Units (HU). The MR-ARFI sequence is comprised of a 2DFT spin-echo sequence (TE = 41ms, TR = 500ms, NEX = 1, ST = 3mm, FOV = 20mm x 15mm). The displacement encoding gradients were synchronized with the sonication and encoded the resulting displacement along the ultrasound beam direction [7]. Interrogation spots were 2mm in diameter (1MHz, 19ms, 28W). They were spaced 2mm apart, and swept an area of 14mm x 10mm x 12mm containing the calcification. MR-ARFI images visualized displacement in the x-z plane, perpendicular to the beam direction. A displacement-weighted map was constructed by combining MR-ARFI maps into a single maximum intensity projection (MIP). For SWI phase imaging, a 3D GRE (TE = 6ms, TR = 21ms, NEX = 2, ST = 1.5mm, FA = 30°, BW = 15.63kHz, FOV = 20mm x 20mm) sequence was used to obtain phase maps. The phase maps were unwrapped using a single step Fourier based technique to visualize calcifications [8].

Results

Both SWI phase images and MR-ARFI were able to visualize the calcification. A series of MR-ARFI images shows the change in tissue displacement as the focal spot nears the calcification (Fig 2). The MR-ARFI displacement map reveals the ROI interrogated, and a clear enhancement of the calcification itself (Fig 3a). The SWI image detects the calcification, showing a dipole pattern on the edges of the calcification (Fig 3b). The contrast to noise ratio within the interrogation region of the MR-ARFI displacement weighted map was 61.57 for MR-ARFI and 28.37 for the SWI image. With the technique presented in this study, SWI imaging was more time efficient than raster scanning the MR-ARFI sub-region. However, a single spot interrogation (56s scan time, 1.9% US duty cycle) centered 3mm away from the calcification was also able to visualize it (Fig 2c).

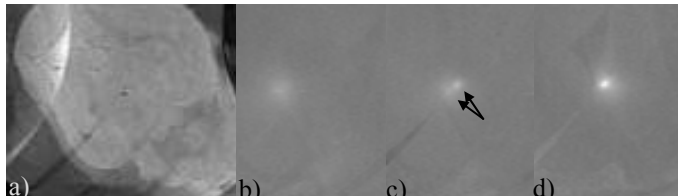


Figure 2. a) MR-ARFI magnitude image. The calcification can be identified as a dropout in the center of the image. b) MR-ARFI displacement map 6mm to the left of calcification c) 3mm to left of calcification, arrows point to interrogation spot and calcification d) within 1mm of calcification.

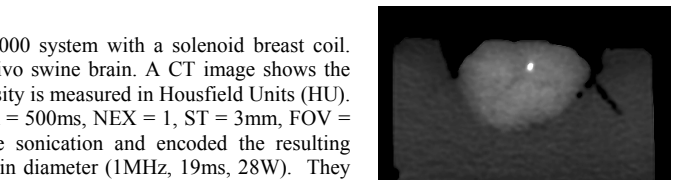


Figure 1. CT (GE 64-Slice High Res) showing experimental setup. The brain was coupled to the ultrasound by a bed of agar gel atop the transducer membrane. The 884 Hu calcification is visible in the brain.

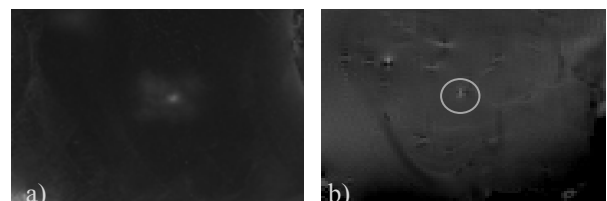


Figure 3. a) MR-ARFI displacement weighted map. The calcification is visible in the center of the MR-ARFI scan volume. b) SWI phase image shows calcification in the circle, other calcifications, and air bubbles present in the ex-vivo swine brain.

Conclusions

MR-ARFI was able to create displacement weighted maps of a 14mm x 10mm x 12mm area inside the brain. The images could be used to sweep a planned ablation area to detect the presence of calcifications. Scan times of MR-ARFI vs. SWI are not immediately comparable since the scan area was arbitrarily chosen to be a reasonably large considering an MRgHIFU brain ablation. Additionally, the sequence presented has not been optimized for time, and a more rapid EPI MR-ARFI technique has been recently developed [9]. This SWI technique can also be further optimized to reduce ambiguity in calcification identification, since other changes in susceptibility may produce similar enhancements. MR-ARFI displacement maps provide a high CNR ratio, and provide specific information about acoustic absorption, as opposed to magnetic susceptibility. Since areas of higher acoustic absorption can cause off focus heating, MR-ARFI may be particularly useful as an alternative or as an adjunct to SWI techniques when preceding an MRgHIFU treatment in the brain. If the general location of a suspected calcification is identified using SWI, an MR-ARFI sweep using only a few sonifications could be sufficient to validate its location.

Acknowledgements

Samantha Holdsworth for discussion on SWI and funding source R21 EB011559

References

- [1] G Gobbi, et al., *Brain Development*, 2004, 27(3):189-200. [2] M Morita, et al., *Neurology*, 1998; 50:1485-1488. [3] E Martin, et al., *Annals of Neurology*, 2009, 66(6): 858-861. [4] FJ Murat, et al., *Cancer Control*, 2007, 14(3):244-9. [5] Z Wu, et al., *JMRI*, 2009, 29:177-182. [6] J Schindler, et al., *Proc of ISMRM 2010*. [7] E Kaye, et al., *Proc of ISMRM 2010*. [8] H Bagher-Ebadian, et al., *JMRI*, March 2008, 27(3):649-652. [9] E Kaye, et al., *MRM, in press*.